JOURNAL OF GEOPHYSICAL RESEARCH, VOL. 92, NO. C12, PAGES 12,993–13,002, NOVEMBER 15, 1987

Processing and Analysis of Large Volumes of Satellite-Derived Thermal Infrared Data

PETER CORNILLON,[1] CRAIG GILMAN,[1] LOTHAR STRAMMA,[2] OTIS BROWN,[3] ROBERT EVANS,[3] AND JAMES BROWN[3]

Reducing the large volume of TIROS-N series advanced very high resolution radiometer–derived data to a practical size for application to regional physcial oceanographic studies is a formidable task. Such data exist on a global basis for January 1979 to the present at approximately 4-km resolution (global area coverage data, ≈2 passes per day) and in selected areas at high resolution (local area coverage and high-resolution picture transmission data, at ≈1-km resolution) for the same period. An approach that has been successful for a number of studies off the east coast of the United States divided the processing into two procedures: preprocessing and data reduction. The preprocessing procedure can reduce the data volume per satellite pass by over 98% for full-resolution data or by ≈84% for the lower-resolution data while the number of passes remains unchanged. The output of the preprocessing procedure for the examples presented is a set of sea surface temperature (SST) fields of 512 × 1024 pixels covering a region of approximately 2000 × 4000 km. In the data reduction procedure the number of SST fields (beginning with one per satellite pass) is generally reduced to a number manageable from the analyst's perspective (of the order of one SST field per day). This is done in most of the applications presented by compositing the data into 1- or 2-day groups. The phenomena readily addressed by such procedures are the mean position of the Gulf Stream, the envelope of Gulf Stream meandering, cold core Gulf Stream ring trajectories, statistics on diurnal warming, and the region and period of 18°C water formation. The flexibility of this approach to regional oceanographic problems will certainly extend the list of applications quickly.

INTRODUCTION

In the past several years, the use of satellite-derived data for oceanographic research has increased dramatically owing to two major developments. First, three satellites carrying sensors of practical value to oceanographers were launched in late 1978. Seasat had a number of active microwave sensors in addition to a visible and infrared radiometer and a passive microwave radiometer (see the special issue on Seasat 1 sensors, *Journal of Oceanic Engineering*, volume OE-5, pages 72–176, 1980). Nimbus 7 [*Madrid*, 1978] was equipped with one sensor designed to measure ocean color for use in chlorophyll-*a* studies and one sensor designed to measure passive microwave radiation. TIROS-N [*Schwalb*, 1978] had the advanced very high resolution radiometer (AVHRR), capable of measuring sea surface temperature (SST) to better than 1°C. TIROS-N was the prototype of the third series of operational polar-orbiting meteorological satellites and has been followed by NOAA 6 through NOAA 10, all carrying an AVHRR or a slightly improved version of this sensor, the AVHRR/2. Digital data from these three satellites became readily accessible soon after their launch; since then a constant stream of digital data has been acquired from the operational satellites in the TIROS-N series. A large volume of the acquired data has been archived by the National Environmental Satellite, Data, and Information Service (NESDIS) of the National Oceanographic and Atmospheric Administration (NOAA) in Suitland, Maryland.

The second major development was the design and encoding of algorithms capable of processing data from these satellites and the emergence of inexpensive 32-bit minicomputers running virtual operating systems on which these codes were implemented. The continued improvements of these software packages with the addition of user-friendly interfaces such as that developed at the Rosenstiel School for Marine and Atmospheric Studies (RSMAS) of the University of Miami has made the integration of satellite-derived data into oceanographic research not only possible but practical and, more importantly, productive. As satellite oceanography has matured, researchers have realized that large numbers of satellite passes are required to detail the spatial and temporal evolution of the phenomena under study. When this became apparent, the groups at RSMAS and the Graduate School of Oceanography (GSO) of the University of Rhode Island (URI) combined their resources to develop an archive of AVHRR passes of the western North Atlantic off the east coast of North America. Since January 1, 1982, an archive of over 6000 AVHRR passes has been acquired; this effort continues with the addition of over 1500 passes per year. For many research projects a small number of the passes have been used at full resolution [e.g., *Lilley et al.*, 1986; *Flament et al.*, 1985]. With the archive in hand, however, it has become apparent that other projects heretofore not undertaken were possible and offered significant scientific contributions if the data in the archive could be reduced to a manageable size of regularly spaced estimates of the SST field in the areas of interest.

In this paper we focus on the strategy of preprocessing and data reduction that we have adopted to this end and briefly discuss several of the more recent applications as examples of the possible uses of the reduced data set. We present only those examples using coarse-resolution (≈4) SST fields. These fields were derived from the high-resolution data in the RSMAS-GSO archive, but they could have been derived as easily from the coarse-resolution global data (≈ 4-km resolution) available from NESDIS. In particular, we note that techniques have been developed to deal with moderate numbers of

[1]Graduate School of Oceanography, University of Rhode Island, Narragansett.
[2]Institut für Meereskunde, Kiel, Federal Republic of Germany.
[3]Rosenstiel School of Marine and Atmospheric Sciences, University of Miami, Florida.

Paper number 7C0669.
0148-0227/87/007C-0669$05.00

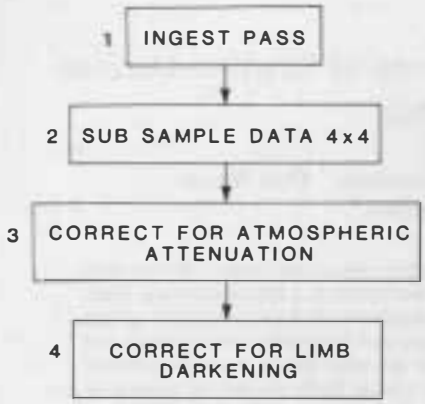

Fig. 1. Preprocessing steps.

satellite passes at full resolution [*Evans et al.*, 1985] but that these techniques are not as readily extended to very large numbers of lower-resolution images. All of the data used were from the AVHRR sensor [*Schwalb*, 1978] carried aboard the TIROS-N satellite series. All the processing was performed using software developed at RSMAS with modifications made at GSO. Some of the processing was performed on the RSMAS VAX 11/780 and the remainder on the GSO VAX 11/750.

Data Analysis

Processing of the data is logically divided into two procedures: preprocessing and data reduction. First, a standard set of algorithms is applied to the data from each pass. This results in an SST value for each pixel in the original pass and a significant reduction in the total volume of data per pass but not in the number of passes in the data set. In the second procedure the number of SST fields in the data set is reduced in one fashion or another depending on the phenomena being studied.

Preprocessing

Figure 1 shows the steps involved in preprocessing, steps common to all of the applications presented below. The data are ingested or read into the computer (step 1 in Figure 1 and Table 1). The data ingested are complete AVHRR high resolution picture transmission (HRPT) passes downlinked (acquired from the satellite in real time) at Wallops Island, Virginia. An HRPT pass consists of the approximately 11 min of data collected by the satellite and immediately transmitted to a ground receiving station while the receiving station is within the field of view of the satellite. Two other data formats are possible from the AVHRR: local area coverage (LAC) data, which are recorded on the satellite and transmitted to a receiving station on command at some later time, and Global Area Coverage (GAC) data, which are processed on the satellite to a reduced spatial resolution, recorded on board, and then downlinked on command to a receiving station. LAC data are similar to HRPT data in all respects except for their remote acquisition; LAC and HRPT data are both collected at the full resolution of the sensor. GAC data are recorded in complete orbits and are of degraded resolution, but in all other respects they are similar to HRPT and LAC data. We return to this point later. As was stated above, all of the processing begins with HRPT data. Although either four or five channels of data are available, only channel 4 for TIROS-N, NOAA 6, NOAA 8, and NOAA 10 or channels 4 and 5 for NOAA 7 and NOAA 9 were used for the processing discussed here; hence only these data were read into the system. All 10 bits were retained in this step. Keeping only one or two of the five channels results in a reduction in the data volume of between 60% and 75% (Table 1).

In the second preprocessing step, only the warmest pixel in each 4 × 4 pixel square was retained. This results in approximately 4-km resolution at nadir (the point directly beneath the satellite) and a reduction in the volume of data remaining after step 1 of over 97% (Table 1). The spatial resolution of the decimated data is similar to that of GAC data. This means that all of the applications discussed below as well as future applications of the same nature could have been accomplished as easily with GAC data. In preprocessing GAC data, step 2 would have been omitted, while all remaining steps in the sequence would have been the same. This is significant, since GAC AVHRR data are available in digital form on a global basis from January 1979 to the present, while HRPT and LAC data are available only for selected regions and periods.

In the analysis of individual passes or small numbers of passes where the location of features from one day to the next is important, the images are carefully navigated (Earth-located). This results in a root-mean-square (rms) uncertainty in the geographic location of any pixel in the image of less than 1.5 km. In the processing described here, careful navigation of the data was not performed because of the fairly coarse resolution resulting from step 2. The location of pixels in the unnavigated images (i.e., using only the estimate of satellite location available from other sources but no manual correction for satellite attitude) was found to vary from satellite to satellite with a maximum rms error for NOAA 7 of 9.6 km (both months in Table 2 are combined for NOAA 7). Thus on the average, even without careful navigation, the location of any pixel in the decimated data is known to within three pixels.

TABLE 1. Data Reduction in Preprocessing Steps

	AVHRR Four-Channel Radiometer		AVHRR/2 Five-Channel Radiometer	
Step	Bits of Data Remaining at End of Step, $\times 10^6$	Percentage of Original	Bits of Data Remaining at End of Step, $\times 10^6$	Percentage of Original
	328.0	100.0	410.0	100.0
1	81.9	25.0	164.0	40.0
2	5.2	1.6	10.5	2.6
3	4.2	1.3	4.2	1.0
4	4.2	1.3	4.2	1.0

TABLE 2. Navigational Accuracy Statistics

Satellite	Month	N	$\overline{\Delta x}$	σ_x	$\overline{\Delta y}$	σ_y
NOAA 6	May 1983	19	2.62	3.16	2.45	6.25
NOAA 6	July 1984	21	2.82	6.84	4.31	4.84
NOAA 7	May 1983	29	−1.18	3.27	4.75	5.38
NOAA 7	July 1984	45	6.98	5.88	0.30	5.09
NOAA 8	May 1983	23	1.73	3.78	1.66	2.35
NOAA 8	July 1984	22	2.24	4.38	0.72	2.18

Following decimation of the data, the *NESDIS* [1982] algorithm, designed to compensate for atmospheric attenuation in the retrieval of SST values from the radiometric data, was applied to the NOAA 7 and NOAA 9 data (step 3 in Figure 1 and Table 1). A review of the theoretical basis and the history of the development of this algorithm as well as a number of forms that the algorithm might take are given by *McMillin and Crosby* [1984]. The input to step 3 consists of two 10-bit data values for each pixel, one for channel 4 and one for channel 5. The output is one 8-bit temperature value for each pixel, hence an additional 60% reduction in the data volume. For TIROS-N, NOAA 6, NOAA 8, and NOAA 10, the channel 4 brightness temperature is simply converted to an equivalent SST value on a pixel-by-pixel basis with no attempt to compensate for atmospheric attenuation. The input in this case is one 10-bit channel and the output is one 8-bit SST value, yielding a 20% reduction in the data volume.

For data from all of the AVHRR sensors, the increased path length through the atmosphere at the edge of a scan line (swath edge) is significantly larger than it is directly beneath the satellite (nadir). This results in a significant depression for retrievals seen at the swath edge, relative to in situ measurements, from both five-channel and four-channel radiometers. Theoretical as well as empirical characteristics of the relationship between the nadir angle to the pixel and the SST are discussed by *Maul* [1983] and *Llewellyn-Jones et al.* [1984]. Basically, because the path length increases inversely with the cosine of the angle between the normal at the pixel of interest and the vector from the pixel to the satellite, the difference between SST retrievals and in situ measures is expected to increase inversely with the cosine of this angle. The coefficient for this cosine term was determined from 212 NOAA 7 retrievals compared with simultaneous, cloud-free in situ observations available from a mooring located at 34°N, 70°W. The equation used was

$$T_s' = T_s + \gamma\left(\frac{1}{\cos\theta} - 1\right) + \zeta \qquad (1)$$

where T_s' is the corrected T_s value; T_s is the derived surface temperature, assuming no scan angle dependence; γ and ζ are constants; and θ is the angle from the normal to the Earth's surface at the pixel of interest. The constants γ and ζ were determined by regressing the satellite-derived values on in situ data obtained from a fixed mooring. The rms deviation of the satellite-derived SST values about the buoy data was reduced from 1.37°C to 0.51°C using this equation with regression values of $\gamma = -2.172$ and $\zeta = 0.623$. (These coefficients were obtained for the western Sargasso Sea and may differ in other regions of the world ocean.) The SST retrievals for all NOAA 7 passes were corrected for limb darkening (step 4 in Figure 1 and Table 1) using (1). This resulted in no reduction in the volume of data but improved the temperature estimates.

The total decrease in the data volume in the first four steps is over 98% for both the four-channel and five-channel radiometers. The results of the preprocessing procedure are saved for further data reduction in the second stage of data processing.

Data Reduction

The first step in the data reduction procedure (Figure 2) consists of remapping all the passes to a common coordinate system. This step does not result in a reduction in the number of SST fields but does result in a reduction in the volume of data; hence it might have been included in the preprocessing group. However, because the output of this step differs from study to study, it has been included here. The actual coordinate system and its center, pixel spacing, and geometric characteristics depend on the study. This step results in an additional reduction of 50% in the volume of data passed from the preprocessing procedure. For all the studies discussed below, the common characteristics of the remapped images are as follows: 512 × 512 pixels, rectangular coordinate system in longitude and latitude, and pixel spacing of between 0.02° ad 0.04° latitude. Note that this yields pixels separated by less than the separation of pixels provided from the previous step, an apparent increase in resolution. In fact, the amount of information has not been increased; pixel values have simply been repeated where necessary by the remapping algorithm. This was done to provide the maximum visual coherence when the images were displayed on the monitor in the processing steps.

The next step differs significantly from study to study. In the applications presented below, three different approaches have been used. They are similar in that they all involve a substantial reduction in the number of images or in the dimensions of the images to be analyzed to a manageable, coherent set. Except for the study of 18°C water formation, each study involves compositing images to reduce the impact of clouds and to develop SST fields at regular intervals. This turns out to be a key step. For studies such as the evolution of the Gulf Stream northern edge, the lack of continuity of the edge along with the irregularly spaced (in time) images made analysis of the data extremely difficult. From the composited data, features emerged that were not readily apparent in visual inspection of the original images.

The compositing of several images consists of retaining the warmest pixel at each location from among the set of images. Because clouds are colder than the SST, this step tends to reduce cloud contamination. In this compositiong step, the scan angle correction is of particular importance.

Details of the data reduction, following remapping of the satellite passes to a common coordinate system, are covered in the discussion of specific applications given below. The additional reduction in the volume of data in these steps exceeds 95% in the four examples presented below.

APPLICATIONS

Gulf Stream Path

For studies of the Gulf Stream path including such phenomena as meandering of the stream, mean path position, ring formation, etc., we have found that 2-day composites retain the important short-term phenomena while at the same time providing a significant reduction in the number of images to be analyzed and decreasing the adverse impact of cloud cover on the analysis. All of the TIROS-N series AVHRR data were

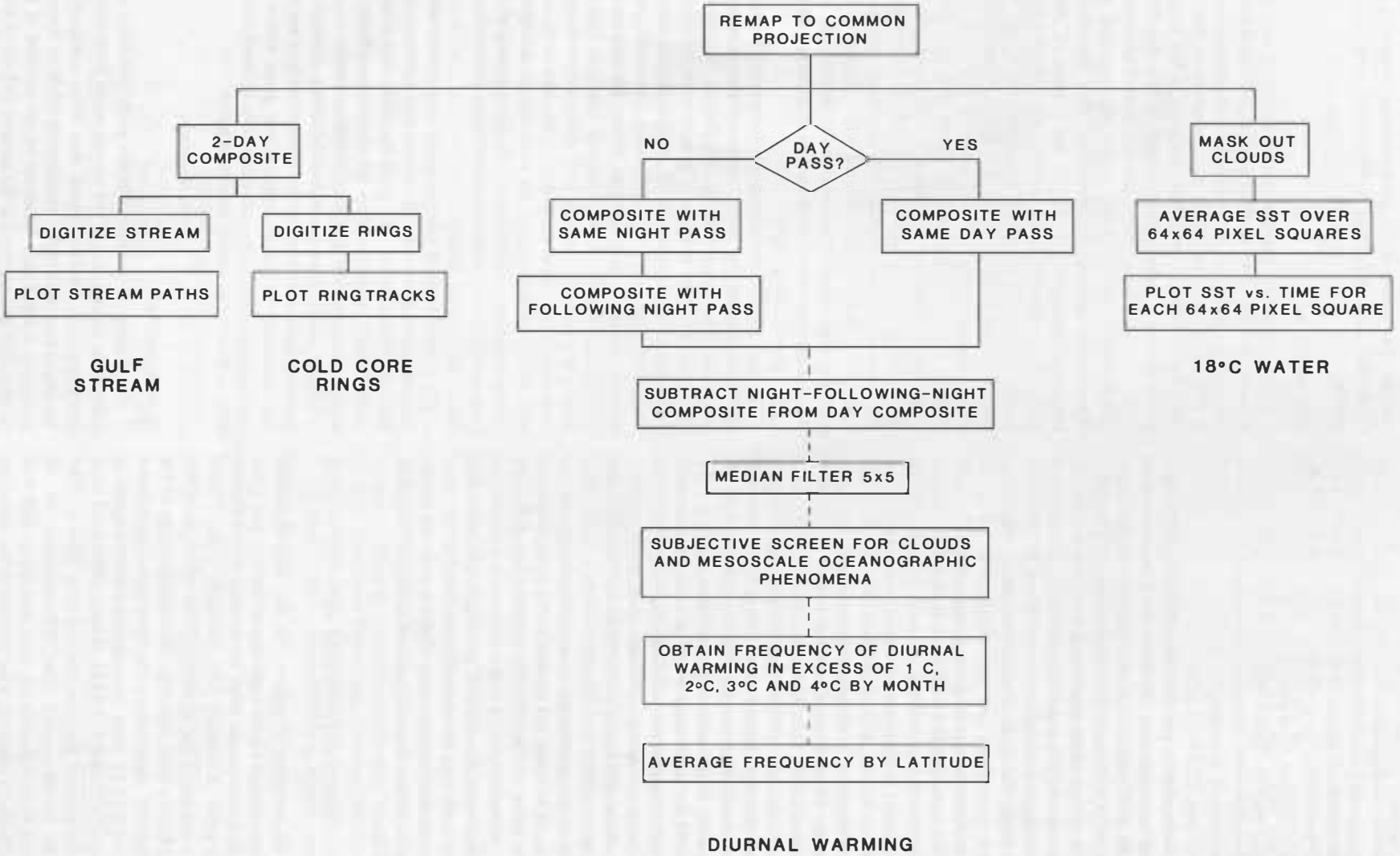

Fig. 2. Data reduction steps.

included in these composites. In general, the RSMAS/GSO archive contains an average of five images per day; hence compositing all the passes over 2 days results in a reduction of 1 order of magnitude. For the period studied, April 1982 through September 1984, the number of SST fields was reduced from approximately 4000 to 408 in this step. Next, the northern edge of the Gulf Stream was digitized subjectively. Subjective location was found to be more accurate than any of the conventional objective algorithms used to locate the Gulf Stream [*Cornillon and Watts*, 1987]. The rms difference between the northern edge of the Gulf Stream east of Cape Hatteras and west of 70°W located subjectively and the location of the 15°C isotherm at 200 m (T_{15}), determined from inverted echo sounders (IES), is less than 15 km [*Cornillon and Watts*, 1987].

Figure 3 shows the positions of the Gulf Stream's northern edge relative to a rhumb line from 36°N, 74°W to 39°N, 60°W for 1982 to 1984. Downstream propagation of meanders is seen throughout the time period. The heavy line extending from April to December 1983 shows such a meander. The two changes of slope of the line represent changes in the phase speed of the wave. Large meanders that break off and form Gulf Stream rings (discussed in more detail below) are also evident, e.g., at 69°W in April 1984. The continuity of the data is evident, with long breaks only in August 1983 and February 1984 for the western half of the region. For the eastern half, which exhibits more extensive cloud cover and lower thermal contrast, breaks in continuity appear during the first and last several months of 1983.

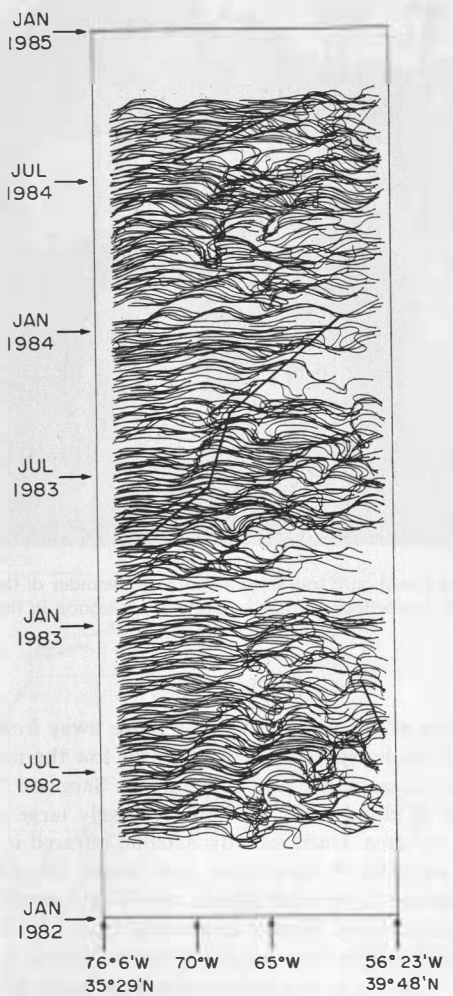

Fig. 3. Positions of the Gulf Stream northern edge relative to a rhumb line from 36°N, 74°W to 39°N, 60°W from 1982 to 1984 [*Cornillon*, 1986]. One realization is plotted for every 2 days.

The data have been replotted in Figure 4 to display the envelope of northern edges. The 1982 data show an envelope wider than that of 1983. The 1982 data also show a quasi-permanent meander (at 38°N, 66°W; evident in the mean track, the white line), which is not present in 1983. The data of the two years have some similarities. For example, all frames of Figure 4 exhibit a relative minimum in the width of the envelope at approximately 70°W.

Contrary to previous perceptions, the data indicate that there is no significant increase in the envelope of meandering from 68° to 58°W [*Cornillon*, 1986]. This is evident in each year plotted and also in all 30 months combined. *Cornillon* [1986] also shows that the convolution within the envelope continues to increase downstream of the New England Seamounts at nearly the same rate as it does upstream. The data indicate that the impact of the New England Seamounts on Gulf Stream meandering appears to be small statistically.

Cold-Core Ring Tracks

Using the same data set compiled for Gulf Stream path studies, the trajectories of cold-core Gulf Stream rings were determined. The 2-day composites allowed for continuity in the tracking of cold-core rings, even more so than in determining the Gulf Stream path. The lack of continuity in the indivvidual images had made the tracking of cold-core rings difficult or impossible, depending on the time of year, the age of the ring, and its distance from the Gulf Stream.

Cold-core rings form when southern meanders of the Gulf

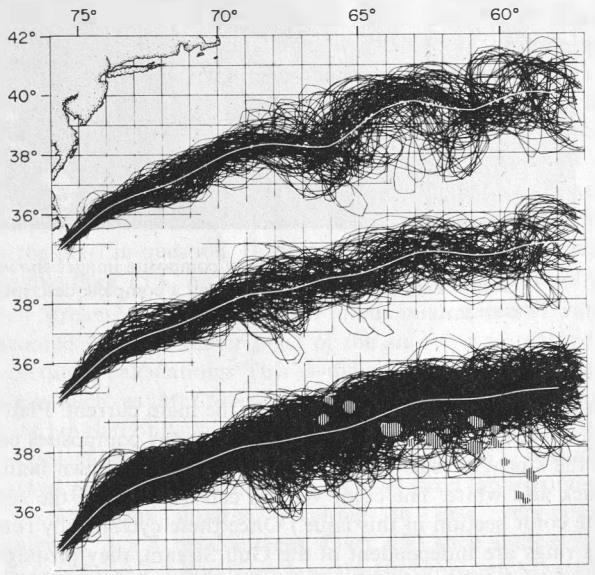

Fig. 4. Gulf Stream northern edges as in Figure 3, but superimposed on one another, for (top) April 19 to December 31, 1982, (middle) all of 1983, and (bottom) April 19, 1982, to September 30, 1984 [*Cornillon*, 1986]. The grey spots on the bottom plot represent water shallower than 3000 m (i.e., the New England Seamounts). The white line in the middle of each set represents the mean track for that set.

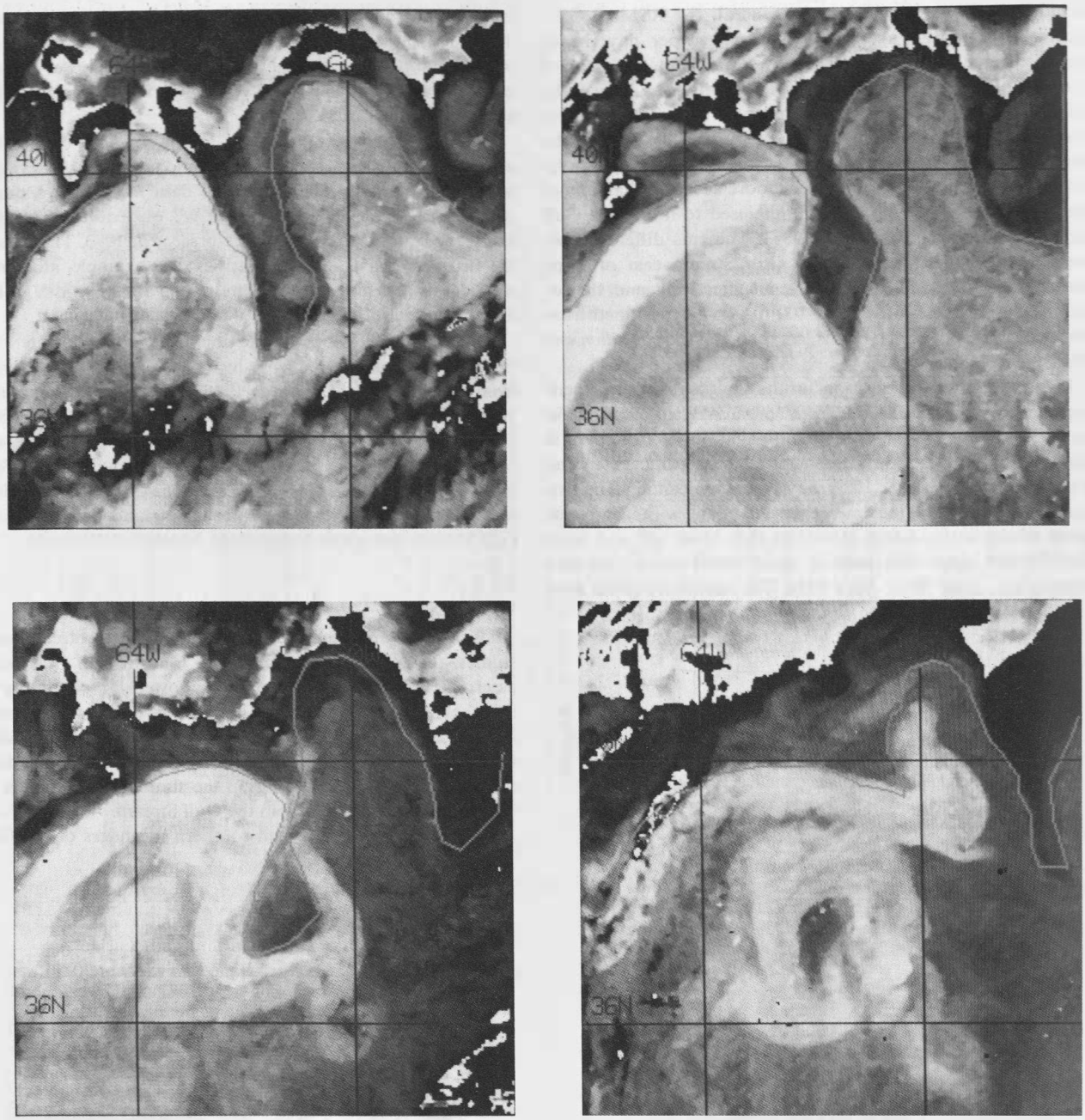

Plate 1. Sequential two-day composite images showing formation of a cold-core ring from a southern meander of the Gulf Stream. (The color version and a complete description of this figure can be found in the separate color section in this issue.)

Stream pinch off and separate from the main current. Plate 1, a sequence of images obtained from the 2-day composites used in the study, reveals such an event. (Plate 1 is shown here in black and white. The color version can be found in the separate color section in this issue.) Once these cyclonically rotating rings are independent of the Gulf Stream, they propagate through the Sargasso Sea for up to several years [*Lai and Richardson*, 1977]. The rings later decay under the following mechanisms: dispersion, instability, interaction with mean flow, small-scale friction, and heat exchanges [*Ring Group*, 1981]. It has been estimated that five to eight cold-core rings form each year [*Lai and Richardson*, 1977], with up to 10 rings drifting in the Sargasso Sea at any one time.

Tracking cold-core rings as they move away from the Gulf Stream is made especially difficult by the low thermal contrast between the rings and the surrounding Sargasso Sea water, intermittent cloud cover, and the relatively large number of rings in the area. Until recently, satellite infrared imagery has proven valuable in identifying only newly formed rings or rings adjacent to the Gulf Stream, which have entrained warm Gulf Stream water around themselves [*Lai and Richardson*, 1977]. Although at the time that a ring is formed, the thermal contrast between it and the surrounding water is high, it is soon capped with a relatively warm layer that substantially decreases the thermal contrast. When the contrast is weak, a clear unobstructed view of the entire ring is required to identi-

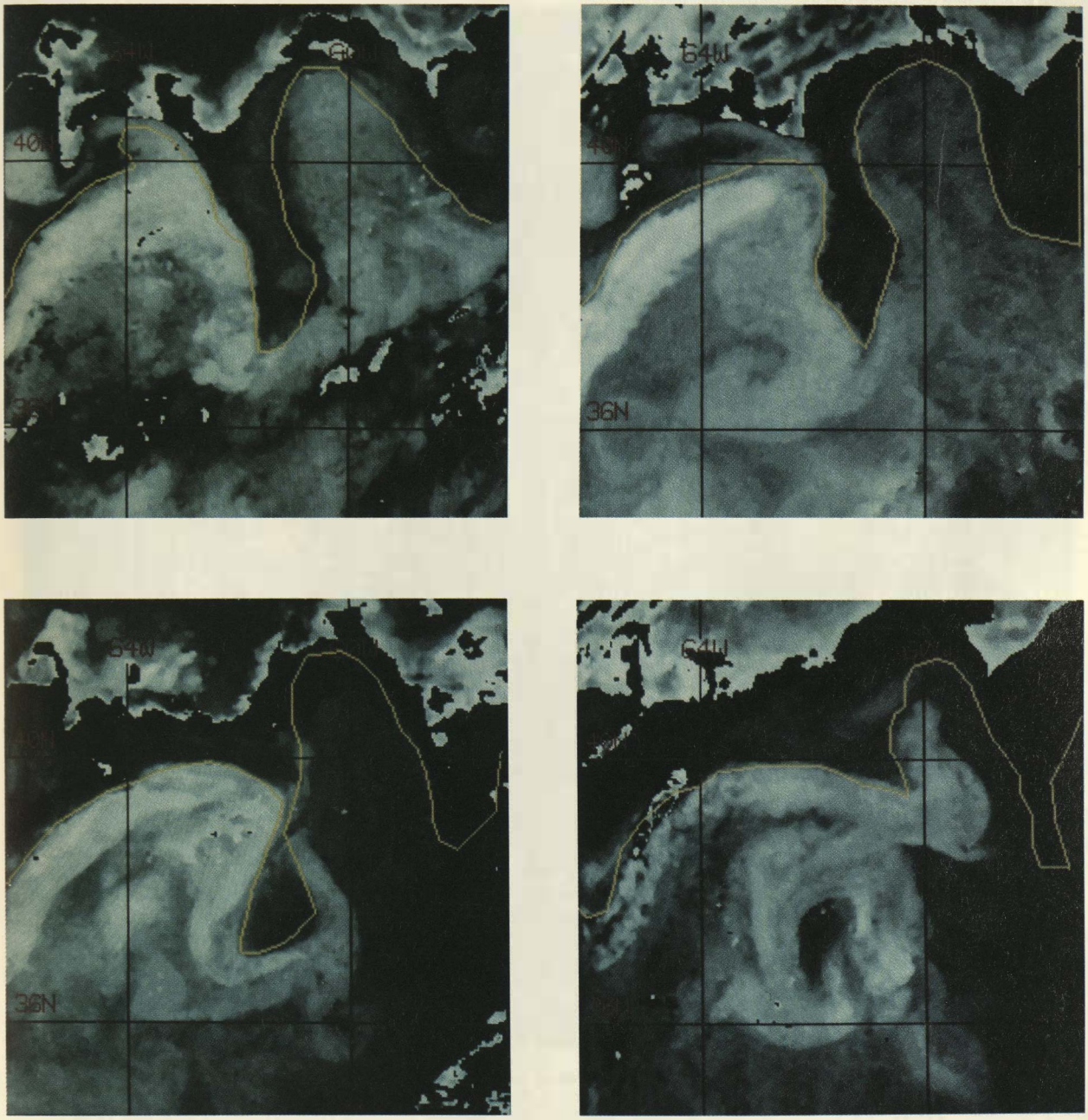

Plate 1 [*Cornillon et al.*]. Sequential 2-day composite images showing formation of a cold-core ring from a southern meander of the Gulf Stream. The northern edge of the Gulf Stream is outlined in yellow.

fy it in satellite-derived SST fields. Because clouds often obscure parts of the ring, such clear views are rare. This results in detection of a given ring at irregularly spaced intervals (weeks). Given the relatively large number of rings in the region and the long intervals separating observations, it becomes difficult or impossible to associate a given observation with a given ring. The compositing of images described above often shortens the interval of time between "clear" views of the ring, thus allowing for the association of an observation with a previously detected ring. This has enabled us to determine long-term tracks of the ring's positions. Figure 5 shows cold-core rings tracked between April 1982 and November 1984. While the general movement of the rings is to the southwest, specific tracks often deviate in direction and frequently make complete reversals. For example, one ring (Figure 5, inset), which formed in June 1982, made several abrupt reversals in direction. After leaving the Gulf Stream, the ring traveled to the west from 65° to 69°W with an average speed of approximately 5 km/d. It then attached itself to the Gulf Stream and traveled in an anticyclonic loop. Once again free of the Gulf Stream, the ring propagated between 68° and 72°W at a uniform speed of 12 km/d. This speed is higher than the previous estimated maximum speed of cold-core rings [*Lai and Richardson*, 1977]. The ring later attached itself to the Gulf Stream twice more before decaying.

The rings we observed rarely traveled in a uniform direction throughout their life cycle. Only a few failed to attach to the Gulf Stream and consequently reverse direction. One notable exception is a ring which formed in April 1982, traveled due south, circled to the east around Bermuda, and then drifted southwest across the Sargasso Sea (Figure 5).

Diurnal Warming

Day-night SST differences in excess of 3°C under conditions of very low wind and high solar insolation have recently been reported by *Stramma et al.* [1986] using a small number of full-resolution satellite AVHRR passes. In a second study, *Cornillon and Stramma* [1985] obtained statistics on the location and frequency of occurrence of such events in the western Sargasso Sea. Because the SST retrievals possible from an instrument with two spectral channels in the 10- to 12-μm atmospheric window are superior to those with only one channel [*McMillin and Crosby*, 1984], only data from the NOAA 7–borne AVHRR were used. Figure 2 (center) shows the data reduction steps for diurnal warming studies. The remapped images, centered on 29°N, 67.5°W and with a grid spacing of 0.044° latitude and 0.050° longitude, are composited into daytime images and nighttime images. Consecutive pairs of nighttime composites are then composited and subtracted from the intervening daytime composite. The result is an estimate of the day-night SST difference for the given day in one image per day, a reduction of about 66% in the number of images. These images were then screened manually (the only subjective step) to eliminate extraneous day-night SST differences resulting either from incorrect temperature retrievals at the edge of clouds in one or more of the passes or from the displacement of mesoscale oceanographic features such as rings or the edge of the Gulf Stream. SST differences were then binned in 1°C intervals between 1° and 5°C (day warmer than night). The final step consisted of counting the fraction of times each month that a given pixel showed diurnal warming in excess of 1°, 2°, 3°, and 4°C. The result for July 1982 is shown in Plate 2. (Plate 2 is shown here in black and white. The color version can be found in the separate color section in this issue.) The analysis was performed for the summers (April through September) of 1982 and 1983 [*Cornillon and Stramma*, 1985].

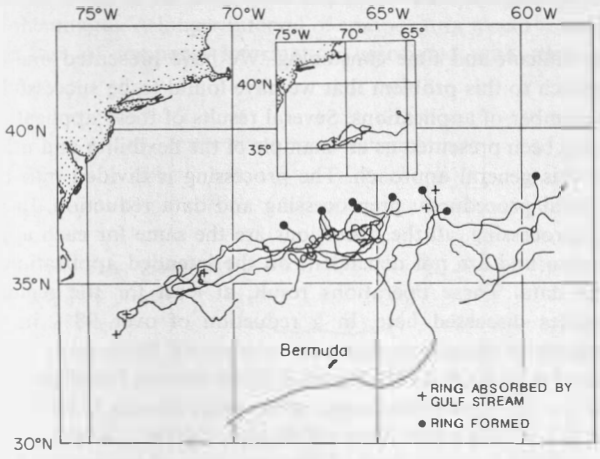

Fig. 5. Long-term tracks of cold core rings between April 1982 and November 1984. The inset shows the track of one ring which formed in June 1982.

Formation of 18°C Water

A further application of this method of data processing relates to the region and time during which 18°C water (or Subtropical Mode Water) is formed. The analysis performed thus far is for the winter and spring of 1983. Of the examples presented, this is the only one in which the images were not composited in one fashion or another. The starting point was the same as for the diurnal warming work, i.e., only NOAA 7 passes resulting from the preprocessing step were used. The data were remapped to a coordinate system rectangular in longitude and latitude and centered on 35.5°N, 66.5°W (Figure 2, right). The grid spacing used was 0.030° of latitude and 0.037° of longitude. Each pixel therefore represents an area of about 11 km^2. Because good SST estimates are critical to this study and because clouds depress the temperature, it is necessary to mask clouds where possible. An SST value was removed as possibly cloud contaminated on the failure of one of two statistical tests made on the 3 × 3 pixel square centered on the pixel in question. If the mean SST value of the square was less than 15°C, an unrealistic value for areas south of the Gulf Stream, or if the maximum minus minimum SST values exceeded 2°C, the center pixel of the square was masked in subsequent calculations. This is different from algorithms of others such as *McClain et al.* [1985] or *Kelly and Davis* [1986] in that only the SST values were used as opposed to all spectral channels. In the next step the mean SST, excluding masked pixels, was calculated in 64 × 64 pixel (approximately 215 × 215 km) squares, resulting in new very-coarse-resolution, 8 × 8 pixel images. Over 450 such images were obtained for the period from January 1983 through May 1983. The mean SST for each of the new pixels was then plotted as a function of time. Figure 6 shows the plots of 35 such time series for pixels seaward of the Gulf Stream. The time series were smoothed with a 3 × 3 median filter. Comparisons of the resulting smoothed SST time series with in situ surface temperature measurements show that the satellite-derived SST

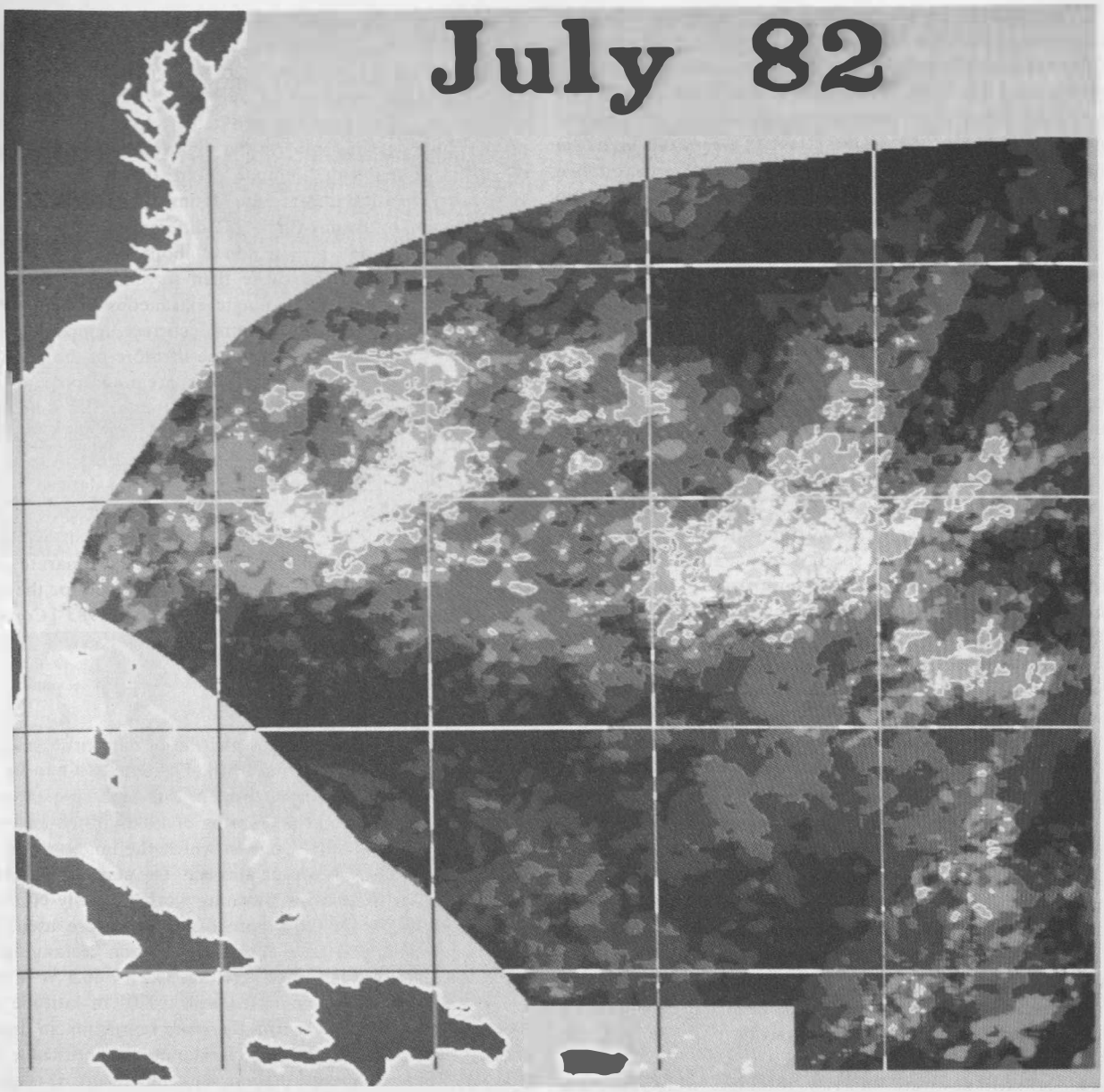

Plate 2. Probability distribution map of dirunal warming in excess of 1°C for July 1982. (The color version and a complete description of this figure can be found in the separate color section in this issue.)

values represent very well the surface temperature of the western Sargasso Sea.

Note the decrease in SST for the square centered at 36°28′N, 58°18′W (Figures 6 and 7) from more than 20°C on January 1, 1983, to 18°C on February 15 and then the increase in SST beginning on April 20 and continuing to the end of the record. From February 15 through April 20 the SST in this area remained very slightly below 18°C; hence 18°C water formation would have been possible for this period. Satellite-derived SST fields are an ideal way to observe 18°C water formation, since ships are not able to collect data covering large horizontal scales repeatedly over extended periods of time.

CONCLUSION

The task of applying the large volume of satellite data currently available to regional oceanographic problems can often be difficult and time consuming. We have presented one approach to this problem that we have found to be successful in a number of applications. Several results of these applications have been presented as an example of the flexibility and utility of this general approach. The processing is divided into two logical procedures: preprocessing and data reduction. In the preprocessing, all the operations are the same for each application and are not dependent on the intended application of the data. These operations result, at least for the regional studies discussed here, in a reduction of over 98% in the volume of data, from numbers such as 10^8 bytes for a 3-year set of over 4000 AVHRR passes of the western North Atlantic to 2×10^6 bytes. The output of the preprocessing is SST fields of 512×1024 pixels covering an area of 2000×4000 km. The important consideration in preprocessing is the reduction in resolution to pixels separated by approximately 4 km in the along-scan and across-scan directions at nadir. This resolution

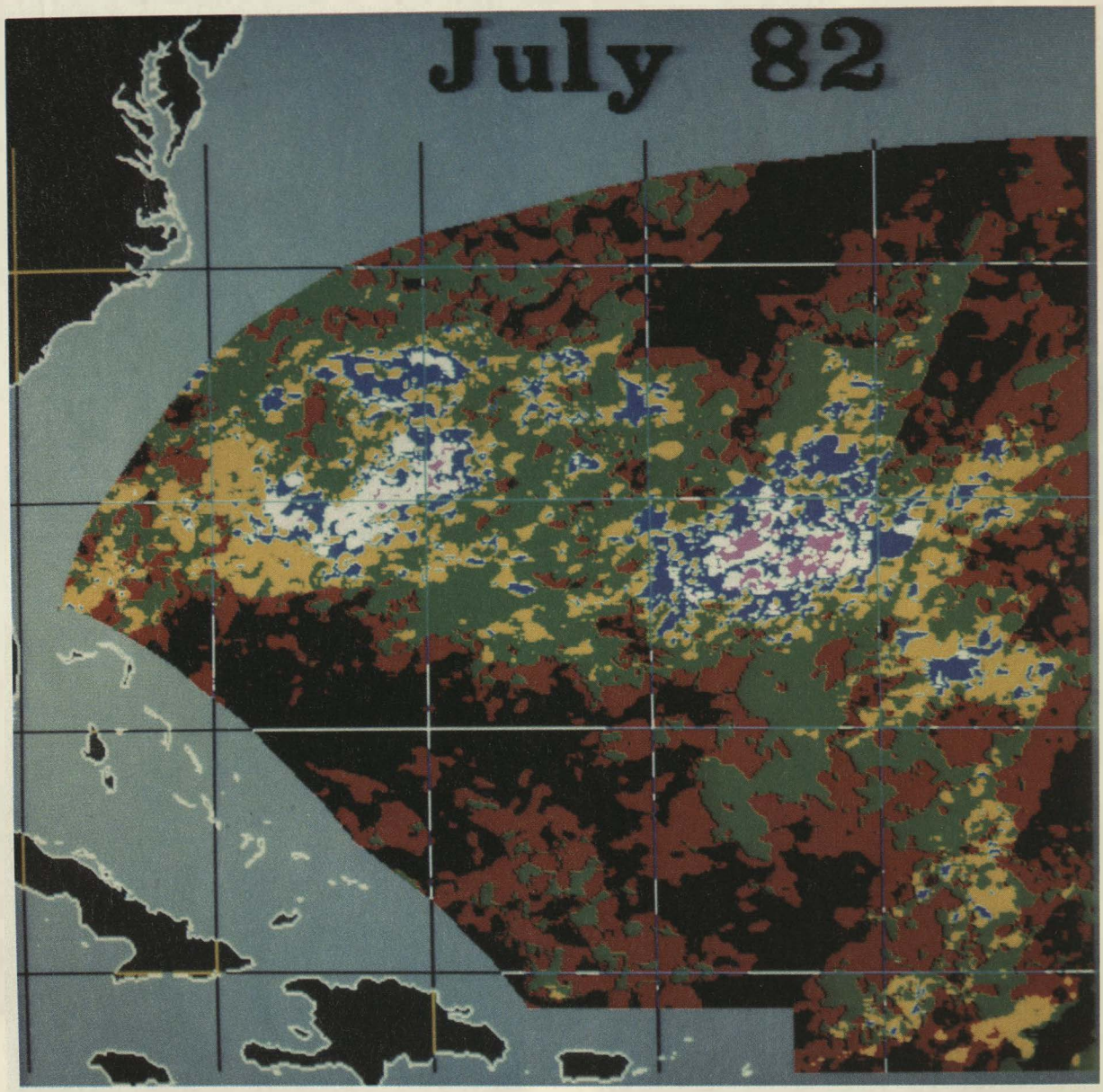

Plate 2 [*Cornillon et al.*]. Probability distribution map of diurnal warming in excess of 1°C for July 1982. The color key is grey for the masked area, black for 0%, red for 1%–5%, green for 6%–10%, yellow for 11%–15%, blue for 16%–20%, white for 21%–25%, and pink for more than 25%. The horizontal grid lines represent 20°, 25°, 30°, and 35°N from bottom to top. The vertical grid lines represent 60°, 65°, 70°, and 75°W from right to left.

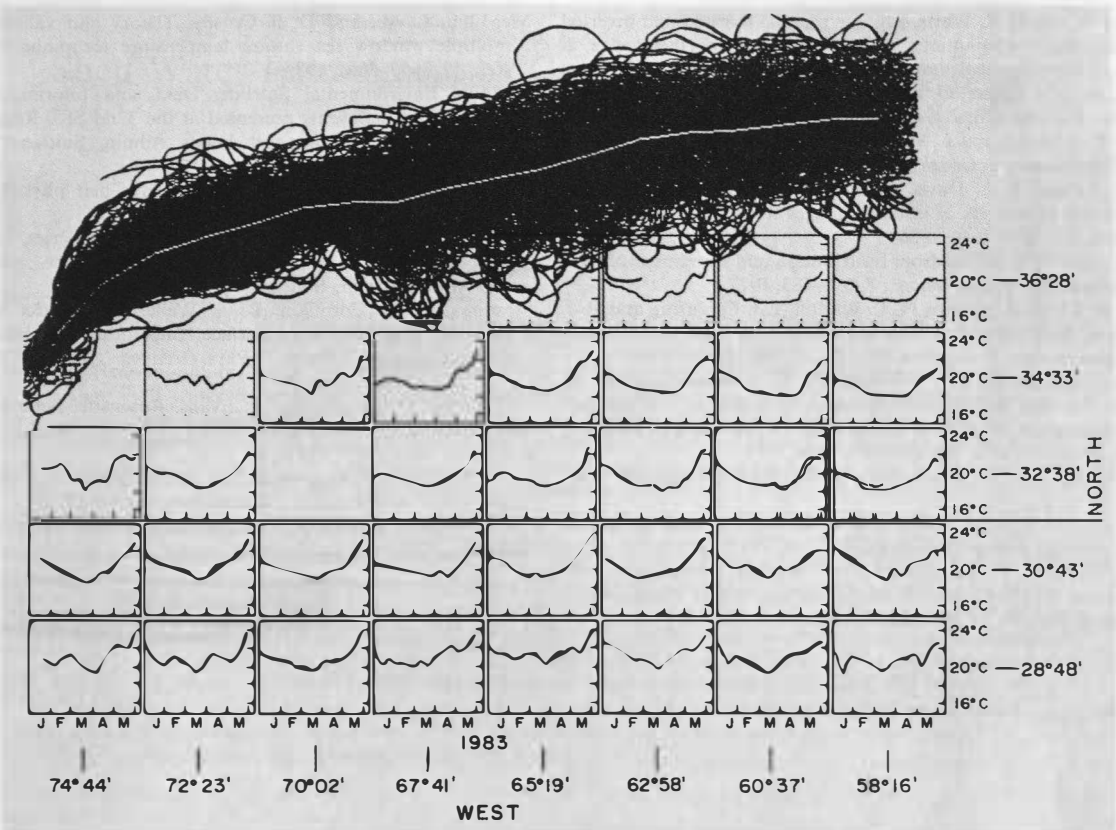

Fig. 6. Time series plots for 35 pixels seaward of the Gulf Stream in 1983. Gulf Stream tracks for April 1982 through September 1984 are included as a reference.

is sufficiently fine for the applications discussed while at the same time not so fine that the volume of data retained is unneccessarily cumbersome.

The data reduction steps varied depending on the intended application, but always resulted in a reduction in the number of SST fields in the data set. Except for the work on 18°C water formation, this reduction is accomplished by compositing images into either 1- or 2-day sets. For the study of Gulf Stream path dynamics and of cold-core ring trajectories, 2-day composites appear to be appropriate, since the scales of motion associated with the 4-km spatial resolution are retained, while at the same time clouds are often composited out of the images. A longer interval of compositing would result in the loss of temporal information associated with the Gulf Stream, while shorter intervals would have significantly increased gaps due to clouds. The relatively continuous time series was seen to make a critical contribution toward facilitating interpretation of the data.

Also of importance is the fact that the resolution of data used in our studies is similar to that of GAC data. These data are available globally from January 1979 to the present in the federal archive at NESDIS and can be applied in a fashion similar to that described in this manuscript anywhere on the earth's surface.

In summary, to use the large volume of satellite data for oceanographic studies, the volume of data must be reduced for processing, and the number of SST fields must be reduced for the analyst. Accomplishing both of these objectives will increase the practicality of using satellite data for future oceanographic research.

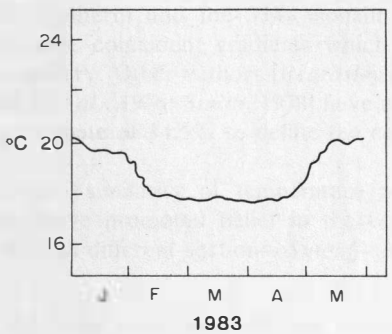

Fig. 7. Magnification of the time series plot in Figure 6 for the pixel centered on 36°28'N, 58°16'W.

Acknowledgments. We are grateful to the Office of Naval Research and to the National Science Foundation for their support of this research through grants N00014-81-C-0062 (ONR) and OCE-8510828 (NSF). The editorial assistance provided by J. Rahn is gratefully acknowledged.

REFERENCES

Cornillon, P., The effect of the New England Seamounts on Gulf Stream meandering as observed from satellite IR imagery, *J. Phys. Oceanogr., 16*, 386–389, 1986.

Cornillon, P., and L. Stramma, The distribution of diurnal sea surface warming events in the western Sargasso Sea, *J. Geophys. Res., 90*, 11,811–11,815, 1985.

Cornillon, P., and D. R. Watts, Satellite thermal infrared and inverted echo sounder determinations of the Gulf Stream northern edge, *J. Atmos. Oceanic Technol.*, in press, 1987.

Evans, R. H., K. S. Baker, O. B. Brown, and R. C. Smith, Chronology of warm-core ring 82B. *J. Geophys. Res.*, *90*, 8803–8811, 1985.

Flament. P., L. Armi, and L. Washburn, The evolving structure of an upwelling filament, *J. Geophys. Res.*, *90*, 11,765–11,778, 1985.

Kelly, K. A., and R. E. Davis, An analysis of errors in sea surface temperature in a series of infrared images from NOAA 6, *J. Geophys. Res.*, *91*, 2633–2644, 1986.

Lai, D. Y., and P. L. Richardson, Distribution and movement of Gulf Stream rings, *J. Phys. Oceanogr.*, *7*, 670–683, 1977.

Lilley, F. E. M., J. H. Filloux, N. L. Bindoff, I. J. Ferguson, and P. J. Mulhearn, Barotropic flow of a warm-core ring from seafloor electric measurements, *J. Geophys. Res.*, *91*, 12,979–12,984, 1986.

Llewellyn-Jones, D. T., P. J. Minnett, R. W. Saunders, and A. M. Zavody, Satellite multichannel infrared measurements of sea surface temperature of the N. E. Atlantic Ocean using AVHRR/2, *Q. J. R. Meteorol. Soc.*, *110*, 613–631, 1984.

Madrid, C. R., The Nimbus-7 users' guide, NASA, Greenbelt, Md., 1978.

Maul, G. A., Zenith angle effects in multichannel infrared sea surface remote sensing, *Remote Sens. Environ.*, *13*, 439–451, 1983.

McClain, E. P., W. G. Pichel, and C. C. Walton, Comparative performance of AVHRR-based multichannel sea surface temperatures, *J. Geophys. Res.*, *90*, 11,587–11,601, 1985.

McMillin, L. M., and D. S. Crosby, Theory and validation of the multiple window sea surface temperature technique, *J. Geophys. Res.*, *89*, 3655–3661, 1984.

National Environmental Satellite, Data, and Information Service, (NESDIS), Coefficients presented at the 32nd SST Research Panel Meeting, Natl. Oceanic and Atmos. Admin., Suitland, Md., Sept. 30, 1982.

Ring Group, Gulf Stream cold-core rings: Their physics, chemistry and biology, *Science*, *212*, 1091–1100, 1981.

Schwalb, A., The TIROS-N/NOAA A-G satellite Series, *Tech. Memo. TM NESS 95*, 75 pp., Natl. Environ. Satell. Serv., Natl. Oceanic and Atmos. Admin., Suitland, Md., 1978.

Stramma, L., P. Cornillon, R. A. Weller, J. F. Price and M. G. Briscoe, Large diurnal sea surface temperature variability: Satellite and in situ measurements, *J. Phys. Oceanogr.*, *16*, 814–826, 1986.

J. Brown, O. Brown, and R. Evans, Rosenstiel School of Marine and Atmospheric Sciences, University of Miami, 4600 Rickenbacker Causeway, Miami, FL 33149.

P. Cornillon and C. Gillman, Graduate School of Oceanography, University of Rhode Island, Narragansett, RI 02882.

L. Stramma, Institut für Meereskunde, Düsternbrooker Weg 20, 2300 Kiel, Federal Republic of Germany.

(Received June 16, 1987;
accepted July 20, 1987.)